Applied Catalysis B: Environmental 166–167 (2015) 270–276

Contents lists available at ScienceDirect

Applied Catalysis B: Environmental

journal homepage: www.elsevier.com/locate/apcatb

Covalently functionalized TiO_2 with ionic liquid: A high-performance catalyst for photoelectrochemical water oxidation

Lin Jing, Min Wang, Xinyuan Li, Ruoyun Xiao, Yufei Zhao, Yuxia Zhang, Yi-Ming Yan*, Qin Wu*, Kening Sun*

Beijing Key Laboratory for Chemical Power Source and Green Catalysis, School of Chemical Engineering and Environment, Beijing Institute of Technology, Beijing, 100081, People's Republic of China

ARTICLE INFO

Article history:
Received 29 September 2014
Received in revised form
20 November 2014
Accepted 23 November 2014
Available online 27 November 2014

Keywords:
TiO_2
Ionic liquid
Photoelectrochemical activity
Water oxidation
Oxygen

ABSTRACT

Ionic liquid (IL) [BsAIm][HSO_4] was covalently introduced to TiO_2 through a simple route. The synthesized IL-TiO_2 hybrid was thoroughly studied by using scanning electron microscopy (SEM), X-ray photoelectron spectroscopy (XPS), Fourier transform infrared spectroscopy (FTIR) and thermogravimetric analysis (TGA). The as-prepared IL-TiO_2 not only exhibits a significantly enhanced photoelectrochemical (PEC) activity, which is almost ten-fold higher than that of the bare TiO_2, but also possesses promising photostability under continuous working conditions. Based on the results, such as charge transfer efficiency, UV–Vis absorption spectroscopy, photoluminescence (PL) emission spectroscopy, and incident-photon-to-current-conversion efficiency (IPCE) tests, we propose a reasonable mechanism to understand the enhanced performance of the IL-TiO_2 toward PEC water oxidation. The significant enhanced PEC performance of IL-TiO_2 should be ascribed to a synergistic effect between covalently linked IL units and TiO_2 particles.

1. Introduction

Photoelectrochemical (PEC) water splitting has attracted tremendous interests due to its separate generation of oxygen and hydrogen gas ($H_2O \rightarrow 1/2O_2 + 2e^- + 2H^+$, $2H + 2e^- \rightarrow H_2$) at the electrodes. It represents an advanced technology of solving the global energy and environmental issues by using the solar energy without producing greenhouse gases or having many adverse effects on the atmosphere [1–8]. However, a kinetic bottleneck for PEC water splitting is the PEC water oxidation, i.e. oxygen evolution reaction (OER), since it requires a total of four holes to form two oxygen-oxygen bonds for the production of one oxygen molecule [9–12].

TiO_2 has been extensively studied as a typical semiconductor photocatalyst for PEC water oxidation due to its excellent photocatalytic activity, high stability, low cost and relatively low toxicity [13,14]. However, the rapid electron–hole recombination severely deteriorates the performance of TiO_2 electrode for PEC water oxidation. To solve this problem, several strategies have been reported, such as integrating TiO_2 with suitable bandgap semiconductors, combining TiO_2 with noble metals as cocatalysts, and coupling TiO_2 with carbon nanomaterial (carbon nanotubes, graphene) or conductive polymer (polyaniline, polypyrrole) [15–22]. Recently, a few studies reported about the use of ionic liquid (IL) as an active unit to modify TiO_2, generating novel photocatalysts with significantly enhanced photocatalytic activity. For instance, Wang et al. showed that the modification with ionic liquid [Bmim]OH could effectively extend the absorption spectrum of TiO_2 to visible-light region [23]. Zhang et al. reported that the photocatalytic activity of BiOI could be enhanced greatly by *in-situ* modification of an IL [Bmim]I (1-buty-3-methylimidazolium iodide) [24].These works essentially indicate that TiO_2 could be rationally modified with suitable IL, resulting novel photocatalyst with desirable PEC performance. Nevertheless, to the best of our knowledge, no study has been reported on the preparation of 1-allyl-3-(butyl-4-sulfonyl) imidazolium hydrosulfate ([BsAIm][HSO_4]) modified TiO_2 hybrid and its utilization as OER photocatalyst for PEC water oxidation.

Herein, we report a simple strategy of synthesize IL [BsAIm][HSO_4] modified TiO_2 (IL-TiO_2) as a novel photocatalyst and investigate its application in PEC water oxidation. We found that the prepared IL-TiO_2 shows remarkable PEC activity and promising photo-stability for water oxidation. Importantly, we proposed a reasonable mechanism to intrinsically understand

* Corresponding authors. Tel.: +86 10 68918696; fax: +86 10 68918696.
E-mail addresses: bityanyiming@163.com (Y.-M. Yan), wuqin_bit@126.com (Q. Wu), bitkeningsun@163.com (K. Sun).

http://dx.doi.org/10.1016/j.apcatb.2014.11.046
0926-3373/

the enhanced PEC performance by performing a careful insight into the electron-hole separation and electron transfer at the surface of the IL-TiO_2. This study could essentially pave a new way for the preparation of functionalized TiO_2 photocatalysts, and consequently find substantial applications in PEC water splitting, as well as in heterogeneous photocatalysis and photocatalytic selective transformations.

2. Experimental

2.1. Materials

Titanium (IV) isopropoxide (TIP, 98%), potassium chloride (KCl), 3-mercaptopropyltrimethoxysilane (MPTMS, 97%), absolute ethanol (>97%), 1-hexadecylamine (HAD, 90%), 2, 2'-Azobis (2-methylpropionitrile)(AIBN), 1,4-Butane sultone, 1-Allyl-1H-imidazole, sulfuric acid were purchase from Sigma Aldrich and used without further treatment.

2.2. Preparation of TiO_2

A typical synthesis of amorphous TiO_2 was as follows [21,25]. 5.3 g HAD was dissolved in 600 mL ethanol, followed by the addition of 2.80 mL KCl solution (0.1 M). Then, 10.2 mL TIP was added under vigorous stirring at room temperature. The resulting white TiO_2 suspension was kept static for 18 h. Then, the amorphous TiO_2 was collected on a Millipore filter, washed with ethanol four times and dried in air at room temperature. Then, 1.2 g of the amorphous TiO_2 was dispersed into a mixture of 10 mL deionized water and 20 mL ethanol. The mixture was sealed within a Teflon-lined autoclave (50 mL) and heated at 90 °C for 20 h. The solid products were collected, washed with ethanol, and dried in air at room temperature.

2.3. Preparation of IL

Synthetic procedure and structure of IL [BsAIm][HSO_4] were shown in Scheme S1. 0.11 mol 1, 4-Butane sultone and 0.1 mol 1-Allyl-1H-imidazole were mixed under vigorous stirring for 72 h. The obtained imidazole ylid solid was washed by aether for 3 times to remove the remaining 1, 4-Butane sultone and byproducts. Then, H_2SO_4 was added under vigorous stirring. The mixture was stirred at room temperature for 72 h, and washed with aether. The mass spectrum of obtained IL was shown in Fig. S1.

2.4. Preparation of IL-TiO_2

To modify IL on the surface of TiO_2, 0.1 g TiO_2 was first dispersed in 200 mL ethanol by sonication for 30 min. Then, MPTMS (2 mL) was added, heated at 50 °C for 1 h, and refluxed at 90 °C for 8 h. MPTMS-treated TiO_2 was sufficiently rinsed with ethanol to wash away any remaining MPTMS moiety. 0.1 g IL, 0.1 g MPTMS-treated TiO_2, 0.002 g AIBN were added into 35 mL acetonitrile solution under vigorous stirring. After mixing for 30 min, the mixture was sealed within a Teflon-lined autoclave (50 mL) and heated at 100 °C for 24 h. Then, the mixture was centrifuged and washed with deionized water and methanol for 5 times to remove any remaining IL and AIBN. The solid products were collected and dried in air at room temperature.

2.5. Structural and morphological characterization

The morphological features of the synthesized powders were characterized by scanning electron microscopy (SEM, QUANTA FEG 250 with an energy dispersive spectrometer). FTIR measurements (Perkin Elmer FT-IR spectrophotometer) were carried out in the transmittance mode in the spectral range 500–2000 cm^{-1} with a resolution better than 0.1 cm^{-1}. UV–vis spectra of bare TiO_2 and IL-TiO_2 were recorded using Shimadzu UV-3600 spectrometer. UV–vis spectrum of IL was measured using Shimadzu UV-2450 spectrometer. Photoluminescence spectra (PL) were acquired at room temperature using a Hitachi FL4600 luminescence spectrophotometer in diffuse reflection mode and with an excitation wavelength of 320 nm.

2.6. Electrochemical and PEC measurements

The working electrodes were prepared as follows: 2 mg of the IL-TiO_2 and 2 mg of bare TiO_2 were dispersed in 1 mL ethanol respectively, by sonication for 10 min to obtain homogeneous suspension. Then, same amount of TiO_2 and IL-TiO_2 (0.5 mL of the suspension) was loaded onto the ITO electrode (1 × 1 cm squares) and dried in air at room temperature. All photocurrent and electrochemical experiments were performed with a CHI 660 electrochemical workstation and conducted in a nitrogen-purged 0.5 M Na_2SO_4 electrolyte solution at pH 7, using the three-electrode setup (particles coated ITO electrode as the photoanode, Hg/Hg_2Cl_2 as the reference electrode, and a platinum wire as the counter electrode). The photocurrent was measured with a bias voltage of 0.25 V. The relationship between the light wavelength and the produced photocurrent on different modified electrodes was studied in the light wavelength range of 300 to 500 nm. The photocurrent was also measured for each switch on/off event under monochromatic light 380 nm irradiation. Linear sweep voltammetry (LSV) was recorded with a sweeping rate of 1 mV s^{-1} in the potential range of −0.2 to 0.8 V vs. Hg/Hg_2Cl_2 under 380 nm light illumination or darkness. The amount of generated O_2 gas was detected by an on-line gas chromatograph (Tianmei GC7900 with a thermal conductivity detector) under the full range of UV-light irradiation. Electrochemical impedance spectroscopy (EIS) was measured in 0.1 M KCl solution containing 5 mM $K_3[Fe(CN)_6]$ by applying an ac amplitude of 5 mV under an open circuit potential in a frequency range from 180 kHz to 0.05 Hz. The incident monochromatic photon-to-electron conversion efficiency (IPCE), plotted as a function of excitation wavelength, was calculated by Eq. (1) [26,27],

$$IPCE\,(\%) = \frac{1240 J_{sc}}{\lambda P_{in}} \quad (1)$$

where J_{sc} is the photocurrent density, λ is the wavelength of the incident light, and P_{in} is the power of the incident light.

3. Results and discussion

3.1. Structural and optical characterization of IL-TiO_2

Scheme 1 illustrates the synthetic procedure of IL-TiO_2 hybrid. Firstly, the hydroxyl groups functionalized amorphous TiO_2 (OH-TiO_2) was prepared according to the procedure reported in a previous work [25]. Then, the OH-TiO_2 was treated in a MPTMS solution, following by a successful generation of hydrosulphonyl groups (—SH) on the surface of TiO_2. The preparation of [BsAIm][HSO_4] was shown in Scheme S1. Finally, the as-prepared [BsAIm][HSO_4] was introduced and combined with TiO_2 through the reaction between C=C of IL and —SH at the surface of TiO_2 to form IL-modified TiO_2.

To investigate the morphology, scanning electron microscopy (SEM) images of the samples were shown in Fig. 1. The prepared amorphous TiO_2 beads exhibited smooth surface, and uniform size with an average diameter of 700 nm (Fig. 1a–c). As comparison, new features were observed on the surface of TiO_2 beads after the modification of IL, as shown in Fig. 1d–f. The IL-TiO_2 sample had rough surface with the adhesion of large quantities of IL. The difference

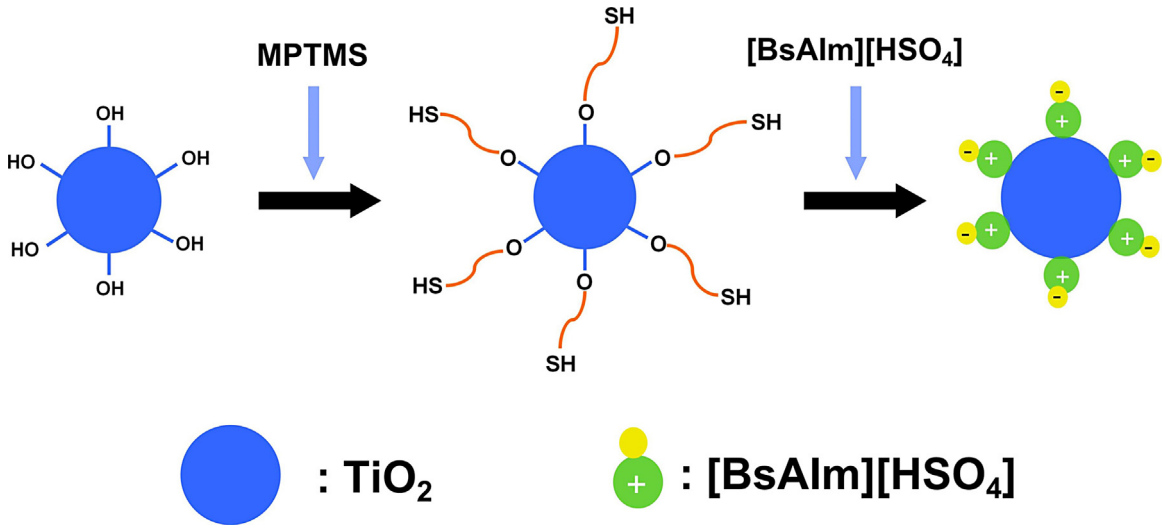

Scheme 1. Illustration of the stepwise synthetic procedure of IL-TiO_2.

of the surface morphologies for TiO_2 and IL-TiO_2 suggests clearly that IL has been successfully introduced to TiO_2. Moreover, Fig. S2a and c showed that the white bare TiO_2 turned to yellow after the modification of IL (Fig. S2b), also implying a combination of IL with TiO_2.

To further confirm the successful introduction of IL on the surface of the TiO_2 particles, Fourier transform infrared spectroscopy (FTIR) spectra were shown in Fig. 2a. For IL, the observed band at 1635 cm^{-1} was attributed to C=C stretching mode. The peaks at 1457 cm^{-1} and 1438 cm^{-1} were assigned to C=N stretching of the imidazole units in IL. In addition, the bands at 1303 cm^{-1} and 1241 cm^{-1} were assigned to C—N stretching of the imidazole units, and peak at 1178 cm^{-1} was associated with S=O stretching mode. Compared with FTIR spectra of IL, the intensity of peak at 1635 cm^{-1} decreased significantly for IL-TiO_2 sample, while a new peak at 692 cm^{-1} appeared corresponding to C—S—C bond. These results strongly demonstrate that IL has been successfully covalently functionalized on the surface of TiO_2. Moreover, obvious shifts at 1126 cm^{-1} and 1241 cm^{-1} may also attribute to the decoration of IL on the surface of TiO_2. X-ray photoelectron spectroscopy (XPS) spectra were performed to investigate the valence states of Ti in TiO_2 and IL-TiO_2 (Fig. 2b). For TiO_2, peaks at 458.1 eV and 463.9 eV were assigned to Ti $2p_{3/2}$ and Ti $2p_{1/2}$ of Ti^{4+} respectively. Interestingly, slight shifts of 0.2 eV toward higher binding energy of both

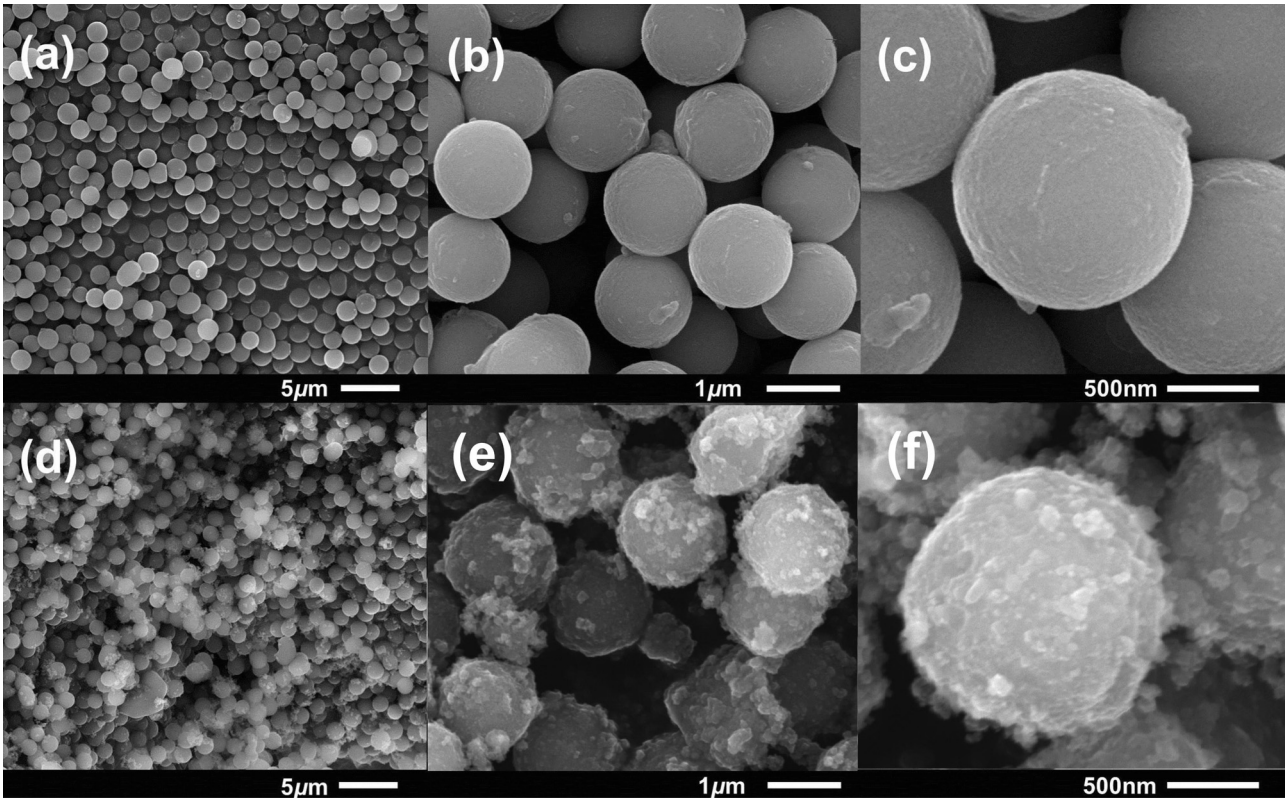

Fig. 1. (a), (b), (c) SEM images of bare TiO_2. (d), (e), (f) SEM images of IL-TiO_2.

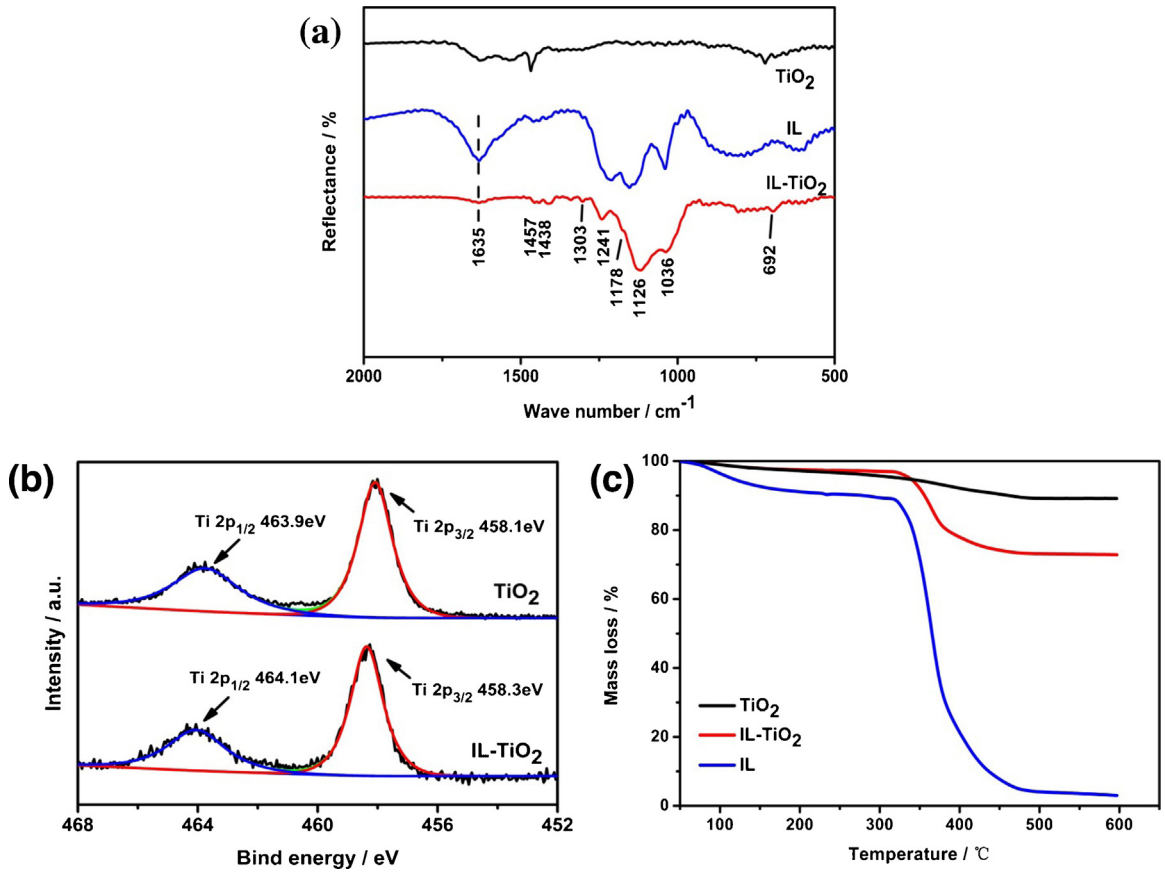

Fig. 2. (a) FTIR spectra of bare TiO_2, IL, and IL-TiO_2. (b) XPS spectra of bare TiO_2, IL, and IL-TiO_2. (c) TGA of bare TiO_2, IL, and IL-TiO_2.

peaks were observed in IL-TiO_2, again indicating a possible formation of chemical bonds between IL and TiO_2. It is expected that such direct bonding between IL and TiO_2 might facilitate the separation of photo-induced electron–hole during the PEC process. To estimate the mass content of IL in IL-TiO_2 hybrid, thermo-gravimetric analysis (TGA) was operated with a heating rate of 10 °C min^{-1} from room temperature to 600 °C under air atmosphere, as shown in Fig. 2c. Below 300 °C, both TiO_2 and IL-TiO_2 showed gradual mass loss. Beyond 320 °C, a much steeper slope, corresponding to the pyrolysis of IL, was observed on IL-TiO_2 compared to TiO_2. About 20% of the initial weight of IL-TiO_2 was lost due to the decomposition of IL, which was obtained by subtracting the weight loss of adsorbed water vapour below 100 °C (5%) from the total weight loss (25%).

To examine the light-absorption properties of samples, UV–vis spectra was obtained and shown in Fig. 3a. It is obvious that IL has high absorption in both UV and visible light region. Compared with pure TiO_2, red-shifts of 50 nm in the absorption edge and 20 nm in the absorption peak (around 360 nm) were observed on the IL-TiO_2 sample. Moreover, IL-TiO_2 sample showed a significantly enhanced absorption in the UV-light region (< 400 nm) and a slight absorption improvement in the visible light range, which can be attributed to the interaction between IL and TiO_2. We noted that the red-shifts and the enhancement of photo absorption imply a better use of solar energy, which should be beneficial for improving the PEC performance of TiO_2. To further verify the effect of IL in electrons transport, electrochemical impedance spectra (EIS), a powerful tool to clarify the electronic and ionic transport properties of semiconductors, was measured under the illumination of UV light (380 nm) at the open circuit potential. As shown in Fig. 3b, IL-TiO_2 hybrid showed a depressed semicircle at high frequencies compared with the pure TiO_2, indicating faster interfacial charge transfer at the surface of IL-TiO_2 than that of pure TiO_2. The obtained results above strongly suggest that the covalent bond between IL and TiO_2 could broaden the absorption wavelength of TiO_2 and enhance the absorptive intensity. Furthermore, the combination between IL and TiO_2 can effectively enhance the separation of photo-induced electron–hole pairs.

3.2. The PEC activity of IL-TiO_2

Due to the enhanced light absorption performance and efficient electron–hole separation, IL-TiO_2 was expected to possess promising performance in PEC application. To verify this, the amperometric I–t curves of both TiO_2 and IL-TiO_2 electrodes were firstly measured in 0.5 M Na_2SO_4 solution under 380 nm light irradiation. In Fig. 4a, both TiO_2 and IL-TiO_2 electrodes showed typical current responses to each switch on/off event. Clearly, the photocurrent of the IL-TiO_2 electrode was much higher than that of TiO_2 electrode, indicating that the photocatalytic oxidation of H_2O into O_2 was greatly promoted by the introduction of IL to TiO_2 surface. Under a visible-light irradiation (430 nm), as expected from the results in Fig. 3a, no photocurrent response was recorded for bare TiO_2 (Fig. S3). In contrast, an enhanced photocurrent response was observed for each switch-on/off event on the IL-TiO_2 electrode, which confirms high photo-activity of IL-TiO_2 under visible light. Linear sweep voltammetric (LSV) of TiO_2 and IL-TiO_2 electrodes were further measured under chopped 380 nm light illumination. Fig. 4b showed the relationship between potential and photocurrent. As seen, low dark current densities were observed at two electrodes, even though the applied potential was as high as 0.8 V. However, under 380 nm UV light illumination, the observed

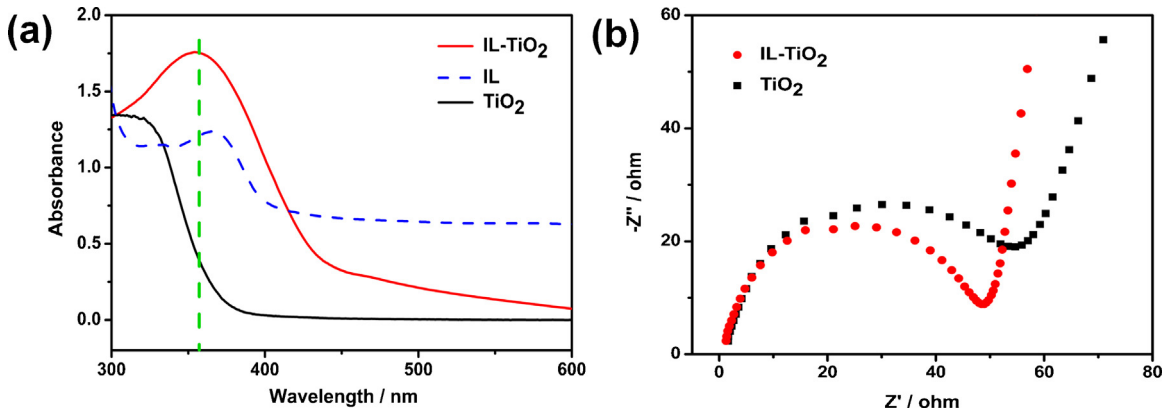

Fig. 3. (a) UV–vis absorption spectra of bare TiO_2, IL and IL-TiO_2. (b) EIS spectra of bare TiO_2 and IL-TiO_2.

photocurrent on IL-TiO_2 electrode increased dramatically along with the increase of potential. It demonstrates strongly that the photo-induced electrons can be effectively driven and successfully separated at positive potential in the condition of illumination. For comparison, the photocurrent of TiO_2 electrode was much lower than that of IL-TiO_2 electrode under the same conditions, implying that IL-TiO_2 possesses much higher activity towards PEC water oxidation than the bare TiO_2. To investigate the effect of light wavelength on the generation of photocurrent, the photocurrent was recorded under different wavelength, as shown in Fig. 4c. It was found that the photocurrent of IL-TiO_2 electrode was significantly higher than that obtained with pure TiO_2 electrode at the whole irradiation wavelength (300–500 nm). The maximum photocurrent of TiO_2 and IL-TiO_2 electrodes were observed under 340 nm and 360 nm light illumination, respectively. The results exactly matched with the UV measurements that their maximum UV–vis absorption was at 340 nm and 360 nm, as shown in Fig. 3a. Durability is another important parameter for evaluating the practical application of catalyst. To this end, we investigated the durability of IL-TiO_2 and TiO_2 toward PEC water oxidation under continuous 380 nm light irradiation. As shown in Fig. 4d, the IL-TiO_2 electrode exhibited high stability even after 10,000 s measurement with a slight decrease of 20% initial current. For comparison, a decrease of nearly 65% of the initial value was observed on TiO_2 electrode.

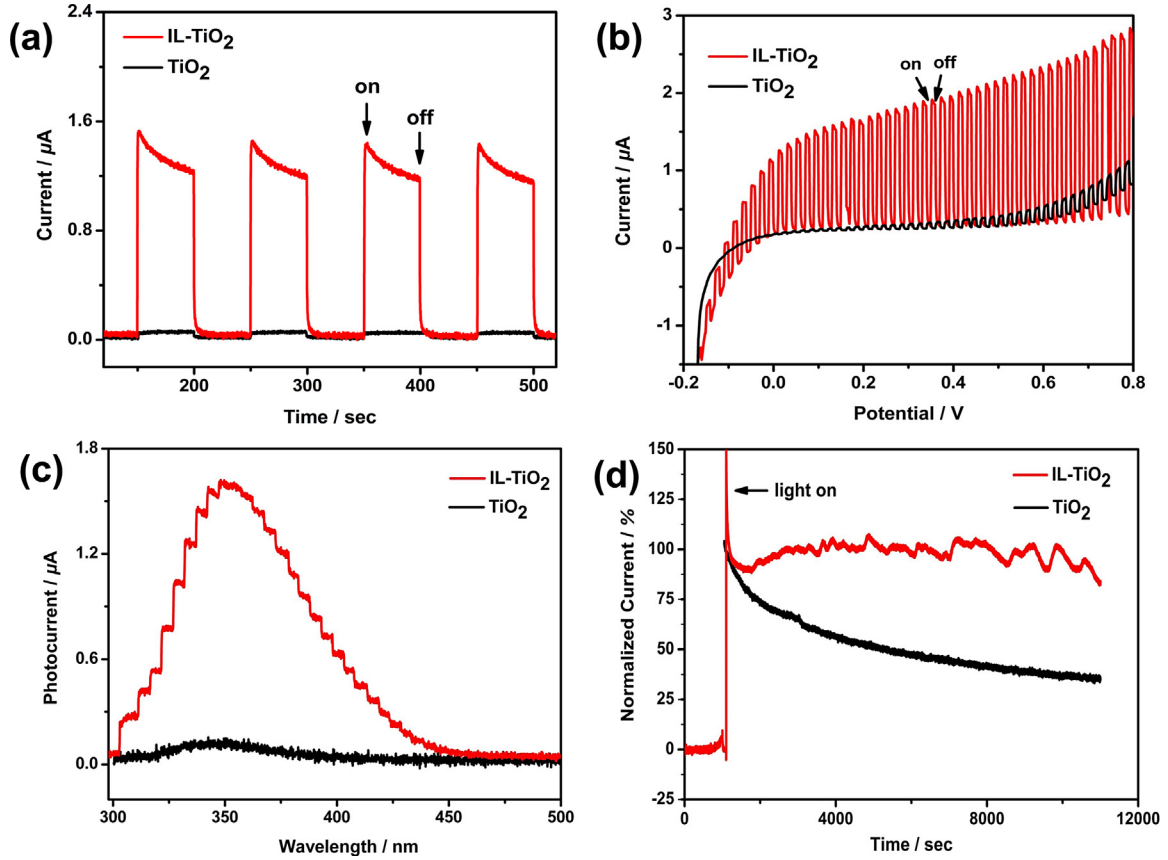

Fig. 4. (a) The photocurrent responses of bare TiO_2 and IL-TiO_2 for each switch-on/off event under 380 nm light irradiation. (b) Linear sweep voltammograms of bare TiO_2 and IL-TiO_2 under 380 nm irradiation at a scan rate of 1 mV/s (with chopping every 10s, range between −0.2 and 0.8 V vs Hg/Hg_2Cl_2). (c) The photocurrent-wavelength curves obtained from bare TiO_2 and IL-TiO_2 modified ITO electrodes in 0.5 M Na_2SO_4 with a bias voltage of 0.2 V. (d) The stability of the PEC oxygen evolution reaction on the bare TiO_2 and IL-TiO_2 electrodes.

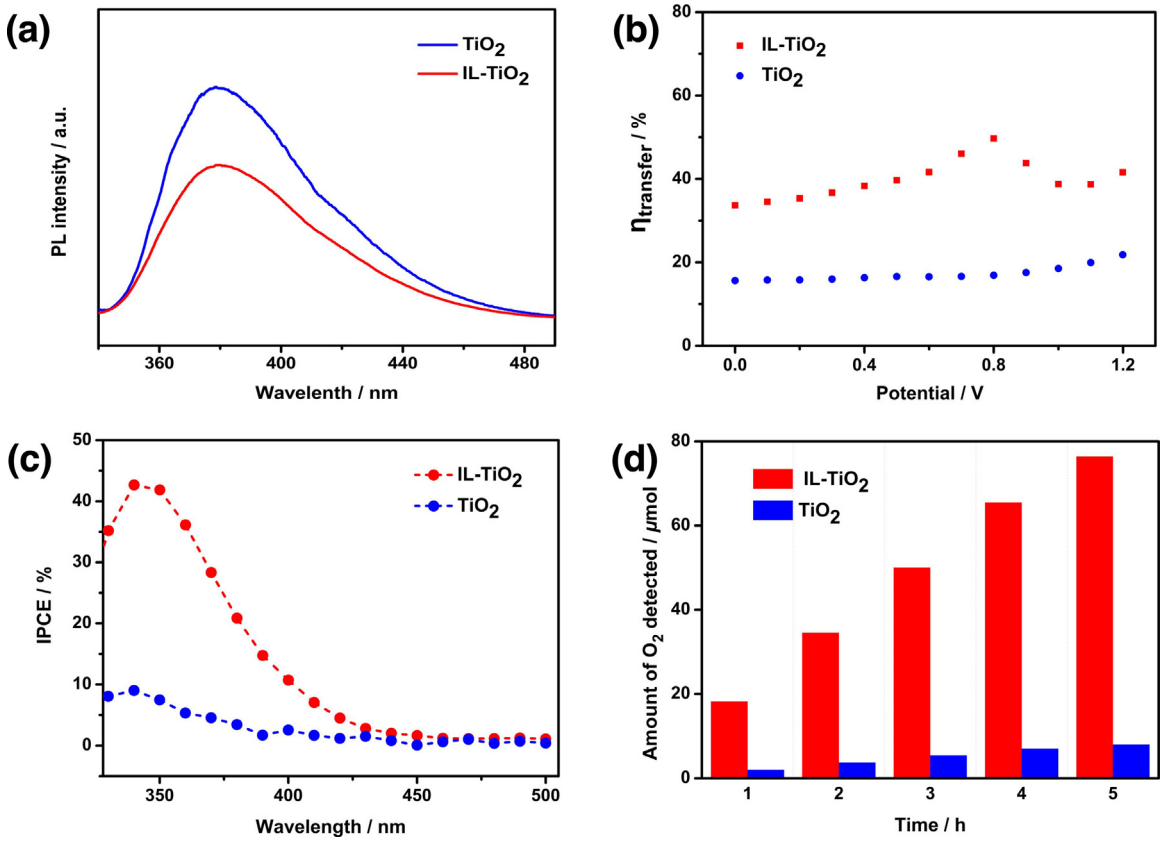

Fig. 5. (a) PL spectra, (b) Charge transfer efficiency, and (c) IPCE spectra of bare TiO_2 and IL-TiO_2. (d) Oxygen evolution over time obtained with IL-TiO_2 and bare TiO_2 electrodes at a bias of 0.25 V under the full range of UV-light irradiation.

The results clearly suggest that the modification of TiO_2 with IL can efficiently improve the durability of TiO_2 towards PEC application.

Charge recombination rate is a critical factor in PEC application. Then, photoluminescence (PL) spectroscope was measured to assess the charge recombination rate of TiO_2 and IL-TiO_2. As shown in Fig. 5a, TiO_2 exhibited a strong and broad PL signal at around 378 nm, while IL-TiO_2 displayed a much weaker peak. The results suggest that introduction of IL on TiO_2 could effectively suppress the undesirable recombination of electrons and holes.

Charge transfer efficiency ($\eta_{transfer}$) can be calculated to assess the utilization efficiency of holes generated on IL-TiO_2. For this purpose, LSV were performed with and without 380 nm light irradiation, as shown in Fig. S4a and b respectively. We used 0.5 M Na_2SO_4 solutions with and without 0.01 M H_2O_2 solution as electrolytes. The $\eta_{transfer}$ was calculated according to Eq. (2).

$$\eta_{transfer} = \frac{I_{(H_2O,light)} - I_{(H_2O,dark)}}{I_{(H_2O_2,light)} - I_{(H_2O_2,dark)}} \quad (2)$$

The key assumption for calculating the $\eta_{transfer}$ is that the oxidation kinetics of H_2O_2 is very fast and charge transfer efficiency on both TiO_2 and IL-TiO_2 are 100% [28]. The relationship between $\eta_{transfer}$ and potential were shown in Fig. 5b. The $\eta_{transfer}$ of IL-TiO_2 was as high as 37% throughout the whole potential range, which is much higher than that obtained on TiO_2 electrode (ca. 15%). The remarkably enhanced $\eta_{transfer}$ for IL-TiO_2 strongly demonstrates an efficient electron-hole separation on IL-TiO_2, which should consequently provide much more holes to catalyse the OER.

We next measured incident-photon-to-current-conversion efficiency (IPCE) of IL-TiO_2 and bare TiO_2 photoanodes. The IPCE of the IL-TiO_2 and bare TiO_2 in the UV region (shown in the Fig. 5c) appeared to be similar to that of the obtained photocurrent-wavelength curves (Fig. 4c). The maximum value of IPCE for the IL-TiO_2 was 42.1%, which is almost 4.5 fold higher than that of the bare TiO_2 (ca. 9.3%). This can be reasonably explained by fact that IL-TiO_2 can absorb more light due to the functionalization of IL because the enhanced light absorption is significantly essential to improve the charge generation efficiency. Furthermore, the IPCE curves clearly showed that IL-TiO_2 electrode owns photocatalytic activity in visible region. By contrast, there was no obvious photocurrent response obtained in the visible region (>400 nm) on the bare TiO_2 electrode. These results confirm that the covalently functionalization of TiO_2 with IL substantially increases visible light absorption, resulting in remarkable increase of IPCE in the visible region.

We finally examined product collected at the anodic electrode. Under a bias of 0.25 V, the generated gas on IL-TiO_2 and bare TiO_2 electrodes were detected using an on-line gas chromatograph. As seen, only O_2 was detected and the amount of generated O_2 under the full range of UV-light illumination over time was plotted in Fig. 5d. It showed that the produced O_2 almost linearly increased with the illumination time for both IL-TiO_2 and bare TiO_2 electrodes. Clearly, the IL-TiO_2 electrode exhibited a significant enhancement in O_2 generation compared with the bare TiO_2 electrode. The obtained results were consistent with photocurrent measurements, confirming strongly that the covalently functionalization of TiO_2 with [BsAIm][HSO_4] could effectively enhance its performance for PEC water oxidation.

3.3. Mechanism on enhancement of PEC activity

Based on the obtained results, we proposed a reasonable mechanism to understand the enhanced PEC performance on IL-TiO_2 (Scheme 2). Under the light illumination, electrons are excited from VB of TiO_2 to CB of TiO_2 to generate electron-hole pairs. While in

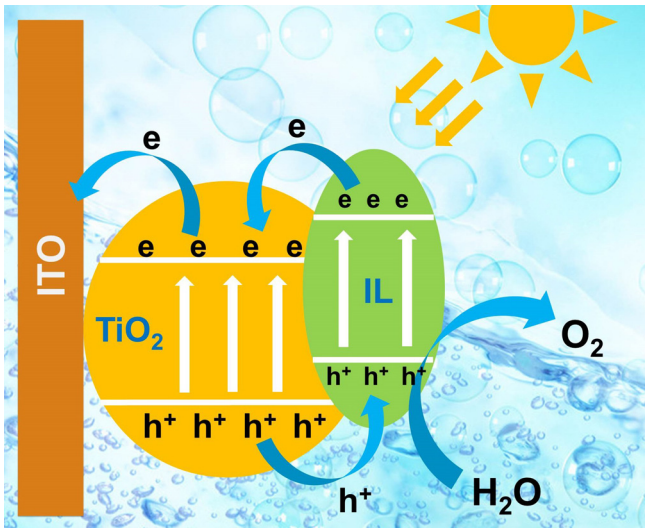

Scheme 2. A proposed mechanism for understanding the enhanced PEC water oxidation at IL-TiO_2 electrode.

the presence of covalently functionalized IL cations on the TiO_2 surface, on one hand, the generated holes in VB of TiO_2 can directly transfer to the HOMO level of IL. On the other hand, more photo-induced electrons could be excited to the CB of TiO_2 due to the electrostatic attraction between the positively charged cations of IL ($[BsAIm]^+$) and the negatively charged electrons. As such, the electrons could be further trapped and transferred to the positively charged ITO electrode, resulting in an efficient charge separation and an easy reaction between the photo-induced holes of IL and water to produce oxygen molecules. Furthermore, the inorganic anions (HSO_4^-) can be dissociated from IL in aqueous solution, which should decrease the pH value of the micro-environment at TiO_2 surface. It is known that electrochemical water oxidation could be facilitated in an acid solution [29] (See the background experiment in Fig. S5). In this work, we choose [BsAIm][HSO_4] as IL, which possessed strong acid properties in aqueous solution to functionalize TiO_2. As a result, it is assumed that such a strategy could essentially create a favourable acid micro-environment at TiO_2 surface and facilitate the oxygen evolution of the PEC water oxidation.

4. Conclusion

In conclusion, we have demonstrated an efficient approach to synthesize IL modified TiO_2 as a novel photocatalyst using for PEC water oxidation. As a proof of concept, [BsAIm][HSO_4] was used as a model IL to modify the TiO_2 bead, resulting in a covalently functionalized IL-TiO_2 composite. A series of measurements, including FTIR, XPS and TGA, have confirmed the electronic interaction and chemical bonding between IL and TiO_2. The resulted IL-TiO_2 shows prominent PEC water oxidation performance, exhibiting ten-fold photocurrent than unmodified TiO_2 under the same conditions and possessing an improved charge transfer efficiency ($\eta_{transfer}$) of 37% compared with that of TiO_2 (ca. 15%). Furthermore, long-term PEC water splitting test also demonstrated the photo-stability of IL-TiO_2 was greatly enhanced. Such an improved PEC activity is believed to ascribe to the synergistic effect between IL and TiO_2, resulting in a high charge separation rate based on the electron transfer and efficient electron extraction. It can be expected that our work will provide new possibilities for using ionic liquid as useful and functional units to complement with TiO_2 and other semiconductors, therefore finding more interesting applications in PEC fields such as water splitting.

Acknowledgments

Financial support from the National Natural Science Foundation of China (Grant no. 21175012, 21006015 and 21070623), the Ministry of Science and Technology (2012DFR40240) and the Chinese Ministry of Education (Project of New Century Excellent Talents in University) is gratefully acknowledged.

Appendix A. Supplementary data

Supplementary data associated with this article can be found, in the online version, at http://dx.doi.org/10.1016/j.apcatb.2014.11.046.

References

[1] A. Iwase, Y.H. Ng, Y. Ishiguro, A. Kudo, R. Amal, J. Am. Chem. Soc. 133 (2011) 11054–11057.
[2] A.J. Cowan, W.H. Leng, P.R.F. Barnes, D.R. Klug, J.R. Durrant, Phys. Chem. Chem. Phys. 15 (2013) 8772–8778.
[3] R. Forgie, G. Bugosh, K.C. Neyerlin, Z.C. Liu, P. Strasser, Electrochem. Solid-State Lett. 13 (2010) D36–D39.
[4] A. Iwase, A. Kudo, J. Mater. Chem. 20 (2010) 7536–7542.
[5] M. Altomare, K., Lee, M. S. Killian, E., Selli, P., Schmuki, Chem.–Eur. J. 19 (2013) 5841-5844.
[6] W.J. Jo, J.W. Jang, K.J. Kong, H.J. Kang, J.Y. Kim, H. Jun, K.P.S. Parmar, J.S. Lee, Angew. Chem. Int. Ed. 51 (2012) 3147–3151.
[7] Q. Peng, B. Kalanyan, P.G. Hoertz, A. Miller, D.H. Kim, K. Hanson, L. Alibabaei, J. Liu, T.J. Meyer, G.N. Parsons, J.T. Glass, Nano Lett. 13 (2013) 1481–1488.
[8] C. Zhen, L.Z. Wang, G. Liu, G.Q. Lu, H.M. Cheng, Chem. Commun. 49 (2013) 3019–3021.
[9] D.K. Bediako, Y. Surendranath, D.G. Nocera, J. Am. Chem. Soc. 135 (2013) 3662–3674.
[10] J. Chen, Y.F. Li, P. Sit, A. Selloni, J. Am. Chem. Soc. 135 (2013) 18774–18777.
[11] J.A. Seabold, K.S. Choi, Chem. Mater. 23 (2011) 1105–1112.
[12] H. Ye, H.S. Park, A.J. Bard, J. Phys. Chem. C 115 (2011) 12464–12470.
[13] S.U.M. Khan, M. Al-Shahry, W.B. Ingler, Science 297 (2002) 2243–2245.
[14] A. Fujishima, K. Honda, Nature 238 (1972) 37–38.
[15] S.H. Elder, F.M. Cot, Y. Su, S.M. Heald, A.M. Tyryshkin, M.K. Bowman, Y. Gao, A.G. Joly, M.L. Balmer, A.C. Kolwaite, K.A. Magrini, D.M. Blake, J. Am. Chem. Soc. 122 (2000) 5138–5146.
[16] T. Tatsuma, S. Saitoh, P. Ngaotrakanwiwat, Y. Ohko, A. Fujishima, Langmuir 18 (2002) 7777–7779.
[17] K. Woan, G. Pyrgiotakis, W. Sigmund, Adv. Mater. 21 (2009) 2233–2239.
[18] M.R. Hoffmann, S.T. Martin, W.Y. Choi, D.W. Bahnemann, Chem. Rev. 95 (1995) 69–96.
[19] Y.J. Xu, Y.B. Zhuang, X.Z. Fu, J. Phys. Chem. C 114 (2010) 2669–2676.
[20] C. Chen, W.M. Cai, M.C. Long, B.X. Zhou, Y.H. Wu, D.Y. Wu, Y.J. Feng, Acs Nano 4 (2010) 6425–6432.
[21] L. Jing, Z.Y. Yang, Y.F. Zhao, Y.X. Zhang, X. Guo, Y.M. Yan, K.N. Sun, J. Mater. Chem. A 2 (2014) 1068–1075.
[22] D. Chowdhury, A. Paul, A. Chattopadhyay, Langmuir 21 (2005) 4123–4128.
[23] S.Z. Hu, A.J. Wang, X. Li, Y. Wang, H. Lowe, Chem. Asian J. 5 (2010) 1171–1177.
[24] Y.N. Wang, K.J. Deng, L.Z. Zhang, J. Phys. Chem. C 115 (2011) 14300–14308.
[25] D.H. Chen, F.Z. Huang, Y.B. Cheng, R.A. Caruso, Adv. Mater. 21 (2009) 2206–2210.
[26] J.H. Bang, P.V. Kamat, Acs Nano 3 (2009) 1467–1476.
[27] Y.-S. Chen, P.V. Kamat, J. Am. Chem. Soc. 136 (2014) 6075–6082.
[28] I.S. Cho, C.H. Lee, Y.Z. Feng, M. Logar, P.M. Rao, L.L. Cai, D.R. Kim, R. Sinclair, X.L. Zheng, Nat. Commun. 4 (2013) 1–8.
[29] Y. Lee, J. Suntivich, K.J. May, E.E. Perry, Y. Shao-Horn, J. Phys. Chem. Lett. 3 (2012) 399–404.